The Ground-State Properties of a New Full-Heusler Alloy Pd$_2$MnPb: DFT+U, QTAIM, and MFA Investigations

A. Adjadj^{a,b,*}, H. Bouafia^c, B. Sahli^c, B. Djebour^c, S. Hiadsi^d and M. Ameri^a

^{a}Laboratoire Physico-Chimie des Matériaux Avancés (LPCMA),
Université Djillali Liabès Sidi-Bel-Abbès, 22000 Algeria

^{b}Department of Physics, Faculty of Matter Sciences, University of Tiaret, 14000 Algeria

^{c}Laboratoire de Génie Physique, University of Tiaret, 14000 Algeria

^{d}Laboratoire de Microscope Electronique et Sciences des Matériaux, Université des Sciences et de la Technologie
Mohamed Boudiaf, Département de Génie Physique, BP1505 El m'naouar, Oran, Algeria

First principles methods have largely contributed in the prediction of new compounds by demonstrating many of their physical properties. This work is based on the same background in which it presents a first prediction of structural properties, the determination of the most stable magnetic ordering, the prediction of energy and mechanical stabilities and the analysis of electronic and magnetic properties of a new Pd$_2$MnPb alloy in the full-Heusler structure. The study of structural properties has allowed the prediction of the lattice parameter, bulk modulus and its pressure derivative of Pd$_2$MnPb in three magnetic orders (non-magnetic, ferromagnetic, and antiferromagnetic). The obtained results for ferromagnetic and antiferromagnetic orders are similar while they are different from those obtained for the non-magnetic one. The comparison between the minima of $E = F(V)$ curves of the three magnetic orders has shown that Pd$_2$MnPb is a ferromagnetic compound. The mechanical stability of this compound has been verified and the results of the elastic constants have shown that this compound has a large elastic anisotropy. The electronic properties have shown that it has a metallic behavior. The Curie temperature has been predicted using mean-field approximation after a calculation of the exchange coupling parameters J_{ij} by spin polarized relativistic Korringa–Kohn–Rostoker method. The obtained results have confirmed the ferromagnetic behavior of this compound. The analysis of bonding natures between the different atoms that form Pd$_2$MnPb has shown that all of them have a strong covalent character.

1. Introduction

Full-Heusler alloys, named after the German engineer Friedrich Heusler [1], have attracted the attention of researchers because of their magnetic and electronic behaviors. Several theoretical and experimental researchers have found that these compounds have physical properties that can be exploited in several fields of application and several industries. Indeed, these compounds are coveted because of their very varied properties such as their ferromagnetic and antiferromagnetic behaviors, metallic character and their rigidities, etc. [2–7].

This family of materials is used in several technical applications such as magnetic devices [8], spin filters [9], optical properties [10], electrical junctions [11] and giant magneto-resistance devices [12, 13] due to their strong magnetic behaviors compared to other compounds of similar structures [2]. The chemical formula of full-Heusler compounds is X$_2$YZ, from which, in most of those synthesized, X and Y are generally magnetic elements that belong to transition metals, actinides or lanthanides, while Z is nonmagnetic [14]. The presence of these magnetic elements is the origin of the strong magnetic behaviors of these compounds, most of which are ferromagnetic.

Mn-based full-Heusler compounds (X$_2$MnZ) belong to this family of materials that are of great importance, the fact which has motivated researchers to determine their properties. Akriche et al. [15] have carried out a complementary study on the elastic, electronic and magnetic properties of Co$_2$MnGe. They have estimated its Curie temperature and have studied its elastic behavior under the effect of the hydrostatic pressure. Using experimental techniques and first-principles calculations, Ahmed et al. [16] have studied the influence of antisite disorder occupancies on the magnetic properties of Co$_2$MnSi. They have found almost equal amount of Mn and Co disorder using neutron diffraction studies. They have also found that these latter results are in a good agreement with those obtained by density functional theory (DFT).

Pd$_2$MnZ-Heusler alloys have very fascinating electronic and magnetic properties because of their ferromagnetic or antiferromagnetic behaviors as well as their

*corresponding author; e-mail: azedine.adjadj@univ-tiaret.dz

metallic nature. Their magnetic moments are mainly due to the partial contribution of Mn-atom, which is generally close to 4 μ_B [17, 18].

DFT based methods, particularly those of the first principles, have largely contributed in the proposition of new compounds by theoretical predictions of their physical behaviors. In this respect, experimenters look for their synthesis because they were fascinated by the results predicted by DFT. In our work, we propose a new compound that is Pd_2MnPb-Heusler starting with the study of its most stable magnetic ordering and the verification of its energy and mechanical stabilities before moving on to the study of its elastic anisotropy and its electronic and magnetic properties.

2. Computational details

Most of results of this work have been obtained by FPLAPW+lo method [19, 20] which is implemented in WIEN2k code [21, 22]. For this method, and to ensure a good accuracy of results in a reasonable time, the choice of input parameters is of great importance. The crystal structure of Pd_2MnPb has been introduced by the atomic positions of the different atoms and the choice of the space group #225.

In Fig. 1 using XCrySDen software [23], we represent respectively the unit-cell and the conventional one of Pd_2MnPb in its full-Heusler structure. The initialization of the FPLAPW+lo-based calculations first begins with a choice of R_{MT} from which the values: 2.1, 2.0, and 22 are respectively chosen for Pd, Mn and Pb atoms. GGA-PBE was chosen for the exchange-correlation functional [24]. To ensure a consistent number of plane waves, a value of $RK_{max} = 8.5$ was used. $l_{max} = 10$ and $G_{max} = 12$ were taken for the maximum value of the partial waves inside atomic spheres and for the largest value of G vector for the Fourier expansion charge. In this work, the choice of k-mesh of the irreducible Brillouin zone (IBZ) [25] is 1500 k-points for the nonmagnetic order, 3000 k-points for the ferromagnetic order and 800 k-points for the antiferromagnetic one. All results have been adopted by a convergence of the total energy with a limit value of 10^{-5} Ry.
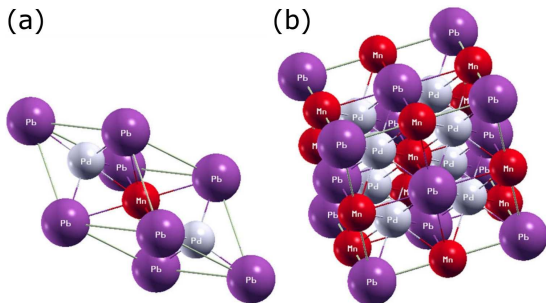

Fig. 1. 3D representation of (a) the unit-cell and (b) the conventional cell of Pd_2MnPb in its full Heusler structure.

In this work, other methods have also been used for the prediction of other physical properties such as the quantum theory of atoms in molecules method (QTAIM) [26, 27], which is implemented in Critic2 code [28, 29] for determining the positions of bonds and spin polarized relativistic Korringa–Kohn–Rostoker method, which is implemented in SPR-KKR package [30, 31], to calculate the exchange coupling parameters J_{ij} for the estimation of the Curie temperature of Pd_2MnPb using mean field approximation (MFA) [32, 33].

For QTAIM method, calculations are based on the results of the total electron density that is obtained by FPLAPW+lo. For a good accuracy of the results and to determine the different critical points (more detail are introduced in the electronic part) for Pd_2MnPb in its most stable magnetic ordering (ferromagnetic) the k-points number has been increased up to 10000.

For SPR-KKR method, the full-potential spin-polarized scalar relativistic approach was used. For the angular momentum cutoff, a maximum value $l_{max} = 4$ was chosen. 750 k-points were used for the mesh of the irreducible Brillouin zone (IBZ). A value of 10^{-5} eV has been adopted as a limit for the convergence of the total energy.

3. Results and discussions

3.1. Most stable magnetic ordering and structural properties

In order to propose a new compound that is not yet synthesized, it is important to determine, in a first time, its structural parameters and its most stable magnetic ordering. Fitting the curve of variation of the total energy as a function of the unit-cell (or conventional-cell) volume $E = F(V)$ by one of the equations of states (EOS) allows the determination of several structural parameters, in particular the lattice parameter, bulk modulus and its pressure derivative. This study also allows the determination of the most stable magnetic ordering focusing on the comparison between the curves of these variations in several magnetic orders (nonmagnetic NM, ferromagnetic FM and antiferromagnetic AFM) from which the most stable order is that which has the minima of the total energy compared with the minima of the other magnetic orders variations.

Figure 2 shows $E = F(V)$ variations in the different magnetic ordering, from which we can notice that FM order is the most stable, leading to that Pd_2MnPb is ferromagnetic. It confirms, therefore, what was mentioned in the introduction that this kind of compounds have a strong magnetic behavior. On the other hand, the different $E = F(V)$ curves have been fitted with Murnaghan equation [34], and the obtained structural results are grouped in Table I. We notice that the total energy of the unit-cell of FM ordering is the lowest which confirms the ferromagnetic behavior of this compound.
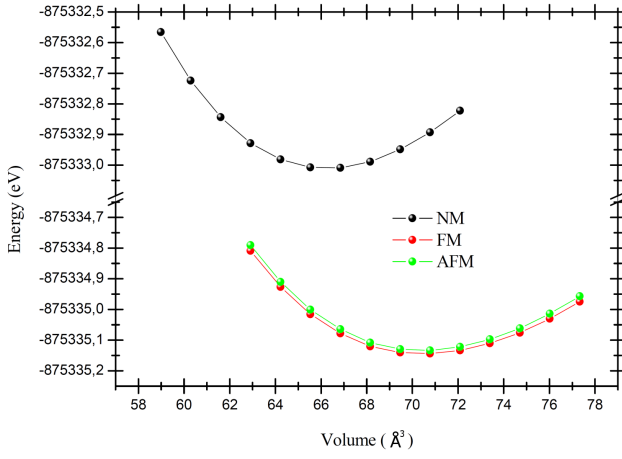
Fig. 2. Variations of the total energy as a function of volume of Pd_2MnPb in nonmagnetic, antiferromagnetic and ferromagnetic orderings.

TABLE I

Calculated lattice constant a_0, Bulk modulus B_0, its pressure derivative B, total unit-cell energy E_0 and cohesive energy E_{Coh} for nonmagnetic, antiferromagnetic and ferromagnetic orderings of Pd_2MnPb.

	a_0 [Å]	B_0 [GPa]	B'	E_0 [eV/cell]	E_{Coh} [eV/cell]
NM	6.4235	140.6189	5.2282	−875333.01080	−11.4057
AFM	6.5562	105.7514	5.8997	−875335.13531	−12.7173
FM	6.5566	101.7953	6.1815	−875335.14546	−13.5404

On the other hand, we note that the values of the lattice parameter and the bulk modulus of FM and AFM orders are similar and far from those obtained for NM one, which confirms the magnetic behavior of this compound. The magnetic behavior of this compound as well as its energy stability can be confirmed by the determination of the cohesive energy. Where, for this compound, its expression is given as the following:

$$E_{Coh}^{Pd_2MnPb} = E_{total}^{Pd_2MnPb} - (2E_{atom}^{Pd} + E_{atom}^{Mn} + E_{atom}^{Pb}).$$
(1)

$E_{total}^{Pd_2MnPb}, E_{atom}^{Pd}, E_{atom}^{Mn}$, and E_{atom}^{Pb} represent respectively the total energy of Pd_2MnPb unit-cell, the atomic energies of Pd, Mn and that of Pb. The obtained results for the cohesive energy of Pd_2MnPb in the various magnetic orderings are grouped in Table I. We note that the obtained values of the cohesive energies are all negative, which confirms the energy stability of this compound in the different magnetic orders but that of FM order is the lowest which confirms once again that Pd_2MnPb full-Heusler is ferromagnetic.

3.2. Mechanical stability and related parameters

It has already been mentioned that Pd_2MnPb full-Heusler has not been synthesized yet. On the other hand, it has been predicted in the structural part that this compound is energetically stable. In this section, we will check its mechanical stability and its elastic behavior as well as its elastic anisotropy. We recall that a compound of cubic structure has three elastic constants noted C_{11}, C_{12} and C_{44}. In this respect, for being mechanically stable it is necessary that their values respond to the Born criteria of mechanical stability which are given by the following expressions [35–37]:

$$C_{11} + 2C_{12} > 0, \quad C_{11} - C_{12} > 0 \quad \text{and} \quad C_{44} > 0. \quad (2)$$

To check the mechanical stability of the Pd_2MnPb, we must first estimate its elastic constants. In this work, their estimation has been made using the theoretical model implemented in IRelast package [38, 39] that is compatible with WIEN2k code. According to this model, their estimation is based on the application of three different distortions D_i on Pd_2MnPb conventional cell; a cubic distortion D_1 to estimate $C_{11}+2C_{12}$, an orthorhombic distortion D_2 to estimate $C_{11}-C_{12}$ and a monoclinic distortion D_3 for the determination of C_{44} (the method is detailed in Refs. [38–41]). These three distortions D_i are based on a chosen range of strains δ, from where in this work strain varies between 2% and −2% to ensure that it is slight enough so that the compound is deformed in the elastic domain only.

The estimation of $C_{11} + 2C_{12}$, $C_{11} - C_{12}$ and C_{44} by the three distortions D_i is realized through the pairing between the polynomial fits of the unit-cell energy variations as a function of the applied strain $E_{Di}(\delta)$ and the theoretical equations of these variations according to the theoretical used model, which are given respectively by [38, 39]:

$$E_{D1}(\delta) = E_0 + V_0\delta(\tau_1 + \tau_2 + \tau_3)$$
$$+V_0\left[\frac{2}{3}(C_{11} + 2C_{12}\delta^2 + O(\delta^3)\right], \quad (3)$$

$$E_{D2}(\delta) = E_0 + V_0[(C_{11} - C_{12})\delta^2 + O(\delta^4)], \quad (4)$$

$$E_{D3}(\delta E_0 + V_0[(2_{C4}4)\delta + O(\delta)], \quad (5)$$

where $E_{Di}(\delta)$, E_0, V_0 and τ_i represent respectively the total energy of the strained unit-cell, that of the unstrained unit-cell, the unstrained unit-cell volume and three parameters related to $\boldsymbol{D}_1$ distortion. In Fig. 3 we show the different $E_{Di}(\delta)$ variations with their polynomial fits. The knowledge of $C_{11} + 2C_{12}$ and $C_{11} - C_{12}$ makes it possible to directly obtain the values of C_{11} and C_{12}. All obtained values of the elastic constants are grouped in Table II from which we can verify that they satisfy the mechanical stability criteria proposed by Born, which makes it possible to predict that Pd_2MnPb is mechanically stable in its full-Heusler structure.

Several other mechanical parameters related to the elastic constants can also be determined including bulk modulus, Young's modulus and shear modulus. Their expressions according to the Reuss and Voigt approximations and their mean values proposed by Hill are respectively given by [42–48]:
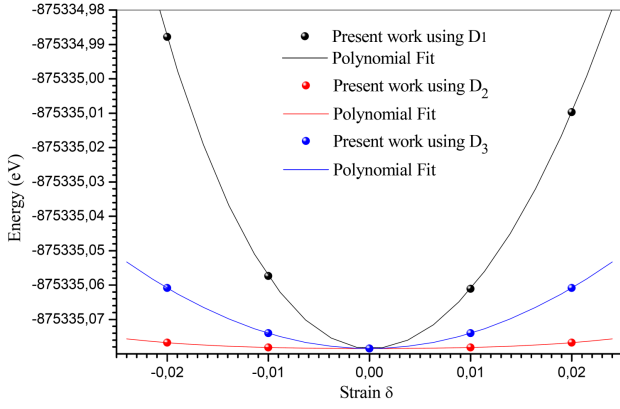
Fig. 3. Variations of the total energy as a function of the applied strains according to the different distortions for Pd$_2$MnPb.

TABLE II

Calculated elastic constants C_{ij} [GPa], Voigt, Reuss and Hill values of: shear modulus G [GPa], Young's modulus E [GPa] and Bulk modulus B [GPa]. The universal elastic anisotropy index A^{U}", Debye temperature θ_D [K], maximum, minimum and average values of Young's modulus $E_{\max}$, $E_{\min}$ and E_A [GPa] of Pd$_2$MnPb.

C_{11}	107.9406	G_H	21.498	A_u	9.6310
C_{12}	97.8557	E_V	86.958	θ_D	179.528
C_{44}	50.0489	E_R	31.709	$E_{\max}$	128.8670
G_V	32.045	E_H	60.229	$E_{\min}$	14.8802
G_R	10.951	B	101.217	E_a	36.9384

$$B_R = B_V = B_H = \frac{C_{11} + 2C_{12}}{3}, \tag{6}$$

$$G_R = \frac{5C_{44}(C_{11} - C_{12})}{3(C_{11} - C_{12}) + 4C_{44}}, \tag{7}$$

$$G_V = \frac{C_{11} - C_{12} + 3C_{44}}{5}, \tag{8}$$

$$E_{R,V,H} = \frac{9G_{R,V,H}B}{G_{R,V,H} + 3B}. \tag{9}$$

Their obtained values are grouped in Table II from which we can deduce that the obtained value for the bulk modulus is very close to that found in the structural part which confirms the precision of this theoretical model and our results. Furthermore for Young's modulus or shear modulus, we notice a very large difference between the value obtained by the Reuss approximation and that obtained by the Voigt approximation, which indicates that this compound has a large elastic anisotropy that will be dealt with in detail in the next section of this work.

The knowledge of the elastic constants and their related mechanical quantities allows the determination of the Debye temperature. This thermodynamic quantity is related to the vibrations of Pd$_2$MnPb atoms because it represents the temperature for which the maximum vibration normal mode is reached. Its determination is realized by the following expression [43–48]:

$$\theta_D = \frac{h}{k_B}\left(\frac{3n}{4\pi}\frac{N_A\rho}{M}\right)^{1/3}V_a, \tag{10}$$

whereby: n, M, h, k_B, ρ, N_A and V_a represent respectively the number of atoms per unit cell, molecular mass, Planck's constant, Boltzmann's constant, the density, Avogadro constant and the average elastic wave velocity. The latter physical quantity V_a is based on the knowledge of the mechanical quantities related to the elastic constants [43–48], from which for its estimation, their Hill's average values have been used. The obtained value of the Debye temperature is shown in Table II.

3.3. Elastic anisotropy

The confirmation of the mechanical stability of this compound allows studying its elastic anisotropy and better understanding its elastic behavior according to the different directions of space. Generally, we can know if a compound is elastically isotropic or anisotropic by analyzing the value of the universal elastic anisotropy index A^U which is given by the following expression [49]:

$$A^U = \frac{5G_V}{G_R} + \frac{B_V}{B_R} - 6. \tag{11}$$

This index is mainly based on the difference between the bulk modulus values and those of the shear modulus which are obtained by the two approximations: that of Reuss and that of Voigt. It can be predicted that a compound is elastically isotropic in case if the value of this index is close or equal to zero. Otherwise it is elastically anisotropic for any value far from zero. We also note that the more the value of this index is far from zero, the more the elastic anisotropy is large. From Table II, A^U found value is very far from zero indicating that Pd$_2$MnPb, in its full-Heusler structure, has a very wide elastic anisotropy.

This index can inform us about the elastic isotropy/anisotropy of Pd$_2$MnPb but it does not allow us to study this behavior according to the three directions of space. For a better understanding of the origin of this large elastic anisotropy and to determine the directions for which this anisotropy is large or small, we have studied the anisotropy of Young's modulus based on the approach proposed by Nye [50]. According to this theoretical approach, for a cubic structure, the variation of Young's modulus according to the different directions of space obeys the following equation [50]:

$$E = \frac{1}{S_{11} - 2\left(S_{11} - S_{12} - \frac{1}{2}S_{44}\right)(l_1^2 l_2^2 + l_2^2 l_3^2 + l_3^2 l_1^2)}. \tag{12}$$

This equation is based on the elastic compliance constants S_{ij} and the direction cosines l_i. Knowing the values of Young's modulus along the three directions of space, this variation can be represented as a closed surface. By analyzing the shape of this surface, we can predict whether the material is elastically isotropic or anisotropic. Hence for an isotropic compound, the value of Young's modulus is invariable in the three directions of space, which gives a surface of a sphere of E radius.
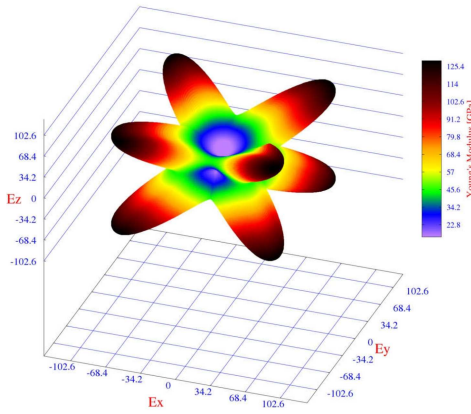
Fig. 4. 3D representation of the directional dependence surface of Young's modulus of Pd_2MnPb.

Fig. 5. 2D projections of the directional dependence surface of Young's modulus according to (001), (110) and (111) planes for Pd_2MnPb.

Contrary to that if Young's modulus is variable, the surface will be deformed and the more it is deformed compared to the spherical form, the more the elastic anisotropy is large.

In Fig. 4 we have plotted the directional dependence surface of Young's modulus of Pd_2MnPb. It can be clearly observed that it is very deformed with respect to a spherical surface which indicates that this compound has a very large elastic anisotropy. This confirms our result obtained by the universal elastic anisotropy index. According to this surface, and according to Table II, the maximum value of Young's modulus E_{max} is very different from that minimal E_{min} because of the large anisotropy of this compound and the average value along this whole surface E_a is very close to that obtained by the Reuss approximation, which confirms the precision of this theoretical model.

To better understand the directions for which the elastic anisotropy is large or small, the directional dependence surface of Young's modulus has been projected according to the most critical planes; (001), (110) and (111) (as shown in Fig. 5). It can be seen that the minimum value is according to (001) and (110) planes, while the maximum value is according to (110) plane. In addition, it should be stated that the directional dependence surface of Young's modulus is too deformed according to (110) plane, which indicates that according to this plane the elastic anisotropy is too large, while this surface is less deformed according to (111) plane, which indicates that the elastic anisotropy is less large according to this plane, but the surface according to this last plane is still far from being circular which indicates that despite of being less deformed, the elastic anisotropy remains always large.

3.4. Electronic and magnetic properties

In the previous sections of this work, we have shown that Pd_2MnPb is mechanically stable in its ferromagnetic ordering. This allowed us to also determine its electronic and magnetic behavio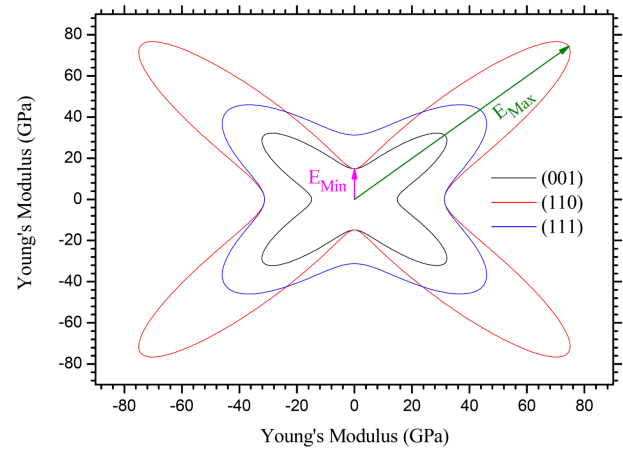rs by studying its electronic band structure and by analyzing the curves of total and partial densities of states. We recall that Pd_2MnPb contains a Mn-atom which has strongly correlated $3d$ electrons. Semilocal functionals do not take into account this strong correlation and give generally erroneous electronic behaviors for this kind of materials [51]. For our compound, and in order to solve this problem, a correction has been added to GGA functional used in this work. This correction is represented by the effective on-site Coulomb interaction parameter U_{eff} (Hubbard's correction) [51]. We have estimated its value by constrained LDA method cLDA described in several previous works [52–54] using the following equation:

$$U_{eff} = E_{Mn\,3d\uparrow}\left(+\frac{1}{2}e\right) - E_{Mn\,3d\uparrow}\left(-\frac{1}{2}e\right)$$

$$-E_F\left(+\frac{1}{2}e\right) + E_F\left(-\frac{1}{2}e\right). \qquad (13)$$

The obtained values of the effective on-site Coulomb interaction parameter U_{eff}, the spin-up eigenvalues of Mn $3d$ states "$E_{Mn\,3d\uparrow}$" as well as those of the Fermi energies related to the addition and the removal of Mn $3d$ electrons are grouped in Table III.

Using GGA and GGA+U, we have obtained the two electronic band structures of Pd_2MnPb that are represented in Figs. 6 and 7 in parallel with the curves of the partial densities of states. We can see from these figures that Hubbard's correction has shifted the spin down peaks of Mn d states of the conduction band to a higher energy level and it has shifted the spin up peaks of Mn d and Pd d of the valence band to a lower energy level with a large change in the shape of the peaks. Despite this correction, it can be seen that there is always an overlap of the bands between the valence band top and the conduction band bottom which shows that this compound is a metal. These figures show that the valence band top and the conduction band bottom are mainly dominated by Mn d and Pd d states. In addition, the great difference

TABLE III

Calculated spin-up eigenvalues of Mn $3d$ states $E_{\mathrm{Mn}\,3d\uparrow}$ [eV] and Fermi energies E_F [eV] corresponding to addition and removal of electrons. The effective on-site Coulomb interaction parameter U_{eff} [eV], Curie temperature T_C [K], total and partial magnetic moments [μ_B] and spin polarization P [%] of Pd_2MnPb

$E_{\mathrm{Mn}\,3d}$ (+0.5e)	$E_{\mathrm{Mn}\,3d}$ (-0.5e)	E_F (+0.5e)	E_F (-0.5e)	U_{eff}	T_C
8.04314	3.45981	10.27733	10.65137	4.95737	172.0033

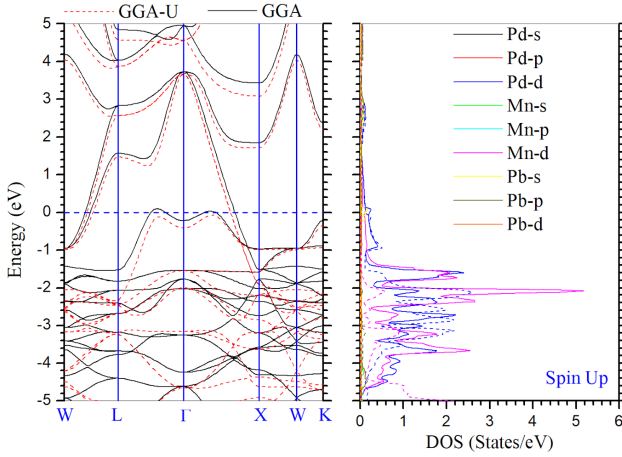| Magnetic moment	Pd	Mn	Pb	Total	Interstitial	P
GGA	0.10337	3.81655	−0.00582	4.32972	0.31223	8.17
GGA+U	0.07439	4.28381	0.00749	4.77921	0.33913	−13.53

Fig. 6. Calculated spin-up electronic band structures and the partial densities of states using GGA (solid lines) and GGA+U (dashed lines) for Pd_2MnPb.
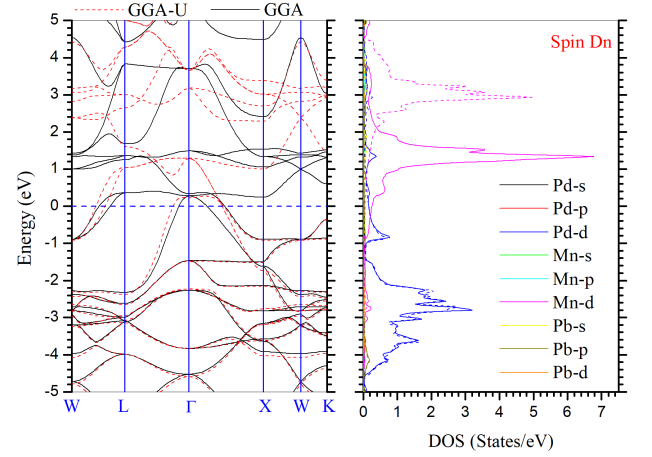

Fig. 7. Calculated spin-down electronic band structures and the partial densities of states using GGA (solid lines) and GGA+U (dashed lines) for Pd_2MnPb.

between the peaks of the both spins shows the strong ferromagnetic behavior of this compound. To confirm this, the spin polarization P has been calculated using GGA and GGA+U using the following expression [40]:

$$P = \frac{\rho\uparrow(\varepsilon_F) - \rho\downarrow(\varepsilon_F)}{\rho\uparrow(\varepsilon_F) + \rho\downarrow(\varepsilon_F)}, \tag{14}$$

where $\rho\uparrow(\varepsilon_F)$ and $\rho\downarrow(\varepsilon_F)$ represent respectively the total density of states near the Fermi level for both spins. From Table III, the spin polarization values obtained by GGA and GGA+U are different from zero and 100%, which confirms the metallic and ferromagnetic natures of Pd_2MnPb. Table III also contains the values of the total, interstitial and partial magnetic moments that have been obtained by GGA and GGA+U, from which it can be stated that the total magnetic moment is large because of the strong ferromagnetic nature of this compound. Furthermore, the great contribution is that of the magnetic moment of Mn-atom, which is about 4 μ_B which also confirms what has already been mentioned in the introduction.

3.5. Estimation of Curie temperature

The most stable magnetic ordering of Pd_2MnPb in its full-Heusler structure has already been determined from which it has been found that it is a ferromagnetic compound. In this section, we have estimated its Curie temperature by mean field approximation (MFA) method [32, 33] using the following equation:

$$\frac{3}{2}k_B T_C^{\mathrm{MFA}} = J_{\mu\nu}^0, \tag{15}$$

in which k_B and $J_{\mu\nu}^0$ represent respectively the Boltzmann constant and the largest eigenvalue of the matrix of the exchange coupling parameters J_{ij} between the different atoms of Pd_2MnPb. As a result, the calculation of the exchange coupling parameters J_{ij} is primordial. In this work, the exchange coupling parameters J_{ij} have been determined by the spin system Hamiltonian of the classical Heisenberg model using spin polarized relativistic Korringa–Kohn–Rostoker (SPR-KKR) code [30, 31]. This latter method makes it possible to calculate the different exchange coupling parameters J_{ij} between the different atoms and also makes it possible to confirm the most stable magnetic ordering of the studied compound. Figure 8 represents the variation of exchange coupling parameters J_{ij} according to the cluster distance, which is centered by Mn atom. It is clearly seen that the Mn–Mn interaction between the two nearest-neighbors is the most dominant and has a positive sign. The second Mn–Mn interaction is also positive and the sum of all Mn–Mn interactions is also positive, which confirms that this compound has a ferromagnetic behavior.
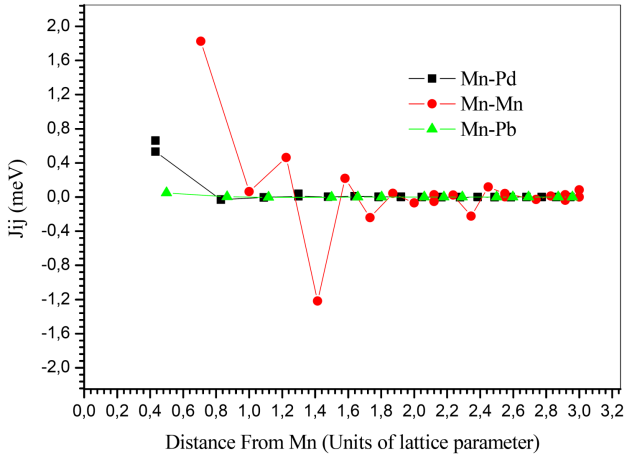
Fig. 8. Variations of the exchange coupling parameters J_{ij} as a function of the cluster distance R_{ij} from Mn (at center) of Pd$_2$MnPb.

Fig. 9. Calculated valence charge density contours and the electron-density gradient vector field along (110) plane of Pd$_2$MnPb. B-letter indicates the positions of bond critical points.

The other interactions between Mn and the other atoms are relatively small contributors in comparison with that of Mn–Mn. On the other hand, all the interactions become negligible for a distance of around $2.5a$, which confirms that the maximum chosen distance of the cluster is largely sufficient. Using Eq. (15) and the values of the exchange coupling parameters that we have determined, the Curie temperature of Pd$_2$MnPb, in its full-Heusler structure, has been estimated (Table III).

3.6. Bonding analysis

The prediction of the bonding types between the atoms that form Pd$_2$MnPb is one of the main objectives of this work. To determine the different positions and the number of bonds between the different atoms that form Pd$_2$MnPb, the QTAIM has been used, while their natures have been predicted by calculating the ionicity factor. QTAIM approach is mainly based on the topological analysis of the electron density in a molecule or a crystal as in our case [26, 27]. According to this approach (QTAIM), the atoms are considered as electron basins separated by surfaces on which the flux of the gradient vector field of the electron density is zero (the projection of these surfaces according to (110) plane is shown by dark lines in Fig. 9). All these characteristics are based on the determination of the critical points CPs of the spatial distribution of the electronic density which are characterized by a zero gradient vector field of the electron density. According to a given direction, the critical point is the position of maximum/minimum of the electronic density and according to this basis that the critical points are classified (bond, cage and ring critical points). What interests us among all these points is the one of the bond (BCP) because it permits to show the presence of the different bonds between the different atoms and consequently, the determination of their numbers and their positions. BCP is the point of the zero flux surfaces,
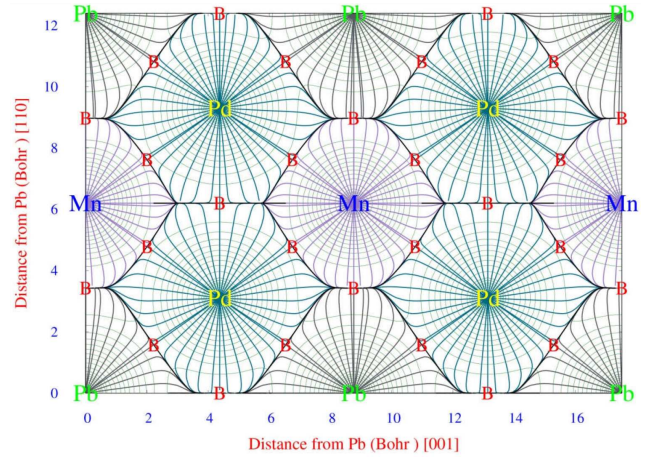
TABLE IV

Calculated positions of Bond critical points BCP and the ionicity factor IF$_{A-B}$ for Pd$_2$MnPb

Bond	BCP Positions	IF$_{A-B}$
Pb–Pd	(0.127, 0.127, 0.127)	0.027
Pd–Mn	(0.386, 0.386, 0.386)	0.100
Pd–Pd	(0.000, 0.250, 0.250)	0.000
Mn–Pb	(0.000, 1.000 , 0.276)	0.025

which separates the bounded atoms, where a single gradient path ($\nabla \rho$(r) trajectory) starting from the nucleus meets another identical path of the other neighboring atom. Figure 9 shows the gradient vector paths of the electronic density that start from the nuclei and reach the zero flux surfaces along the densest plane (110). The different bond critical points (BCPs) are indicated by a B letter. According to this figure, it can be mentioned that the bonds which exist between the different atoms that form Pd$_2$MnPb are: Pb–Pd, P–Pd d, P–Mn d and Mn–Pb. The positions of the different BCPs are shown in Table IV. This table also contains the values of the ionicity factor based on Pauling electronegativities [55] which makes it possible to predict the behavior of a bond between two atoms A and B. Its expression is given by

$$\text{IF}_{A-B} = 1 - \exp\left(-\frac{(\chi_A - \chi_B)^2}{4}\right). \qquad (16)$$

χ_A and χ_B represent respectively the values of Pauling electronegativities of A atom and B atom. A value close to 1 of this factor indicates that the bond between A and B is of ionic character, while a value close to zero indicates a covalent character. From Table IV, all ionicity factor values for the different bonds are close to zero indicating that all bonds have a strong covalent character.

4. Conclusion

The present work is a first prediction of the most stable magnetic ordering, structural, elastic, electronic and magnetic properties of a new full-Heusler compound Pd_2MnPb using mainly FPLAPW+lo method which is implemented in WIEN2k code. The most remarkable conclusions of each property are listed below:

- The results of the structural properties have shown that the values of the lattice parameter for FM and AFM magnetic orders are similar, while they are far from those obtained for NM order, which indicates the strong magnetic behavior of Pd_2MnPb. The analysis of the minima of $E = F(V)$ curves in the three studied magnetic orders has shown that this compound has a ferromagnetic behavior. The cohesive energy values have confirmed these results and they have shown the energy stability of this compound.

- The study of elastic properties has shown that Pd_2MnPb is mechanically stable. The determination of the elastic constants allows the determination of other mechanical quantities such as Young's modulus, shear modulus and the Debye temperature. The prediction of the universal elastic anisotropy index and the analysis of the directional dependence surface of Young's modulus have shown that this compound has a large elastic anisotropy.

- The electronic properties have been determined taking into account the strong correlation between Mn $3d$ electrons by the estimate of the effective on-site Coulomb interaction parameter $U_{\rm eff}$, which has been added to GGA functional as a correction. Despite this correction, the obtained results by GGA and GGA+U have shown that Pd_2MnPb has a strong metallic character. The spin polarization values have confirmed its ferromagnetic behavior. The Curie temperature has been estimated by mean-field approximation MFA using the values of the exchange coupling parameters J_{ij} obtained by SPR-KKR method. The results of the latter have confirmed the ferromagnetic character of this compound. The analyses of the bonds between the atoms that form Pd_2MnPb using QTAIM and the values of the ionicity factor have shown that they have all a strong covalent character.

References

[1] F. Heusler, W. Starck, E. Haupt, *Verh. DPG* **5**, 220 (1903).

[2] K.R.A. Ziebeck, K.U. Neumann, *Landolt-Börnstein*, New Series, Group III, Vol. 32/c, Ed. H.P.J. Wijn, Springer, Berlin 2001, p. 64.

[3] J. Pierre, R.V. Skolozdra, J. Tobola, S. Kaprzyk, C. Hordequin, M.A. Kouacou, I. Karla, R. Currat, E. Lelièvre-Berna, *J. Alloys Compd.* **101**, 262 (1997).

[4] J. Tobola, J. Pierre, S. Kaprzyk, R.V. Skolozdra, M.A. Kouacou, *J. Phys. Condens. Matter* **10**, 1013 (1998).

[5] J. Tobola, J. Pierre, *J. Alloys Compd.* **296**, 243 (2000).

[6] J. Tobola, S. Kaprzyk, P. Pecheur, *Phys. Status Solidi B* **236**, 531 (2003).

[7] M. Gillessen, R. Dronskowski, *J. Comput. Chem.* **31**, 612 (2010).

[8] S. Datta, B. Das, *Appl. Phys. Lett.* **56**, 665 (1990).

[9] K.A. Kilian, R.H. Victora, *J. Appl. Phys.* **87**, 7064 (2000).

[10] K.H.J. Buschow, P.G. van Engen, *J. Magn. Magn. Mater.* **25**, 90 (1981).

[11] C.T. Tanaka, J. Nowak, J.S. Moodera, *J. Appl. Phys.* **86**, 6239 (1999).

[12] J.A. Caballero, Y.D. Park, J.R. Childress, J. Bass, W.-C. Chiang, A.C. Reilly, W.P. Pratt Jr., F. Petroff, *J. Vac. Sci. Technol. A* **16**, 1801 (1998).

[13] C. Hordequin, J.P. Nozières, J. Pierre, *J. Magn. Magn. Mater.* **183**, 225 (1998).

[14] T. Graf, C. Felser, S.S.P. Parkin, *Prog. Solid State Chem.* **39**, 1 (2011).

[15] A. Akriche, B. Abidri, S. Hiadsi, H. Bouafia, B. Sahli, *Intermetallics* **68**, 42 (2016).

[16] S.J. Ahmed, C. Boyer, M. Niewczas, *J. Alloys Compd.* **781**, 216 (2019).

[17] P.J. Webster, Ph.D. Thesis, Sheffield University, 1967.

[18] P.J. Webster, R.S. Tebble, *J. Appl. Phys.* **39**, 471 (1968).

[19] G.K.H. Madsen, P. Blaha, K. Schwarz, E. Sjöstedt, L. Nordström, *Phys. Rev. B* **64**, 195134 (2001).

[20] K. Schwarz, P. Blaha, G.K.H. Madsen, *Comput. Phys. Commun.* **147**, 71 (2002).

[21] P. Blaha, K. Schwarz, G.K.H. Madsen, D. Kvasnicka, J. Luitz, R. Laskowski, F. Tran, L.D. Marks, "WIEN2k, An Augmented Plane Wave + Local Orbitals Program for Calculating Crystal Properties", Karlheinz Schwarz, Techn. Universität Wien, Austria 2018.

[22] P. Blaha, K. Schwarz, P. Sorantin, S.K. Trickey, *Comput. Phys. Commun.* **59**, 399 (1990).

[23] A. Kokalj, *Comput. Mater. Sci.* **28**, 155 (2003).

[24] J.P. Perdew, K. Burke, M. Ernzerhof, *Phys. Rev. Lett.* **77**, 3865 (1996).

[25] H.J. Monkhorst, J.D. Pack, *Phys. Rev. B* **13**, 5188 (1976).

[26] R.F.W. Bader, *Atoms in Molecules. A Quantum Theory*, Oxford University Press, Oxford 1990.

[27] R.F.W. Bader, T.T. Nguyen-Dang, Y. Tal, *Rep. Prog. Phys.* **44**, 893 (1981).

[28] A. Otero-de-la-Roza, E.R. Johnson, V. Luaña, *Comput. Phys. Commun.* **185**, 1007 (2014).

[29] A. Otero-de-la-Roza, M.A. Blanco, A. Martín Pendás, V. Luaña, *Comput. Phys. Commun.* **180**, 157 (2009).

[30] H. Ebert et al., *The Munich SPR-KKR package*, ver. 7.7.

[31] H. Ebert, D. Ködderitzsch, J. Minár, *Rep. Prog. Phys.* **74**, 096501 (2011).

[32] H.E. Stanley, *Introduction to Phase Transitions and Critical Phenomena, International Series of Monographs on Physics*, Oxford University Press, New York 1971.

[33] P.W. Anderson, *Solid State Phys.* **14**, 99 (1963).

[34] F.D. Murnaghan, *Proc. Natl. Acad. Sci. USA* **30**, 244 (1944).

[35] M. Born, *Math. Proc. Camb. Philos. Soc.* **36**, 160 (1940).

[36] F. Mouhat, F.-X. Coudert, *Phys. Rev. B* **90**, 224104 (2014).

[37] M. Born, K. Huang, *Dynamical Theory of Crystal Lattices*, Oxford University Press, Oxford 1954.

[38] M. Jamal, S. Jalali Asadabadi, Iftikhar Ahmad, H.A. Rahnamaye Aliabade, *Comput. Mater. Sci.* **95**, 592 (2014).

[39] M. Jamal M. Bilal, Iftikhar Ahmad, S. Jalali-Asadabadi, *J. Alloys Compd.* **735**, 569 (2018).

[40] S. Mokrane, H. Bouafia, B. Sahli, B. Abidri, B. Djebour, S. Hiadsi, D. Rached, *Chin. J. Phys.* **59**, 625 (2019).

[41] B. Boughoufala, H. Bouafia, B. Sahli, B. Djebour, S. Mokrane, S. Hiadsi, B. Abidri, *J. Supercond. Nov. Magn.* **32**, 4005 (2019).

[42] B. Sahli, H. Bouafia, B. Abidri, A. Abdellaoui, S. Hiadsi, A. Akriche, N. Benkhettou, D. Rached, *J. Alloys Compd.* **635**, 163 (2015).

[43] R. Hill, *Proc. Phys. Soc. A* **65**, 349 (1952).

[44] M.I. Kholil, M.Z. Rahaman, M.A. Rahman, *Comput. Condens. Matter* **13**, 65 (2017).

[45] M.J. Mehl, B.K. Klein, D.A. Papaconstantopoulos,. in: *Intermetallic Compounds: Principles and Practice*, Vol. I, Eds. J.H. Westbrook, R.L. Fleischer, Wiley, 1995.

[46] W. Voigt, *Lehrbuch der Kristallphysik*, Taubner, Leipzig 1928.

[47] E. Schreiber, O.L. Anderson, N. Soga, *Elastic Constants, and Their Measurements*, McGraw-Hill, New York 1973.

[48] B. Mayer, H. Anton, E. Bott, M. Methfessel, J. Sticht, P.C. Schmidt, *Intermetallics* **11**, 23 (2003).

[49] S.I. Ranganathan, M. Ostoja-Starzewski, *Phys. Rev. Lett.* **101**, 055504 (2008).

[50] J.F. Nye, *Physical Properties of Crystals* Clarendon Press, Oxford 1985.

[51] V.I. Anisimov, F. Aryasetiawan, A.I. Lichtenstein, *J. Phys. Condens. Matter* **9**, 767 (1997).

[52] G.K.H. Madsen, P. Novák, *Europhys. Lett.* **69**, 777 (2005).

[53] V.I. Anisimov, O. Gunnarsson, *Phys. Rev. B* **43**, 7570 (1991).

[54] Ch. Spiel, P. Blaha, K. Schwarz, *Phys. Rev. B* **79**, 115123 (2009).

[55] L. Pauling, *The Nature of the Chemical Bond: An Introduction to Modern Structural Chemistry*, 3rd ed., Cornell Univ. Press, Ithaca (NY) 1960.